JOURNAL OF APPLIED POLYMER SCIENCE VOL. 18, PP. 2637–2651 (1974)

Strain Behavior of Particulate-Filled Composites

J. LEIDNER and R. T. WOODHAMS *Materials Research Centre, Department of Chemical Engineering and Applied Chemistry, University of Toronto, Toronto, Ontario, Canada*

Synopsis

A theoretical expression has been derived to describe the strain behavior of rigid plastic composites containing spherical filler particles. By combining the predicted ultimate strength values with the appropriate modulus relationship, the complete stress–strain history and corresponding fracture energy may be estimated. The theoretical predictions were compared with experimental values obtained for a general-purpose polyester resin containing spherical glass beads. The influence of silane coupling agents and filler adhesion was also evaluated. Although the experimental values showed considerable scatter, the general trend agreed fairly well with the theoretical predictions.

INTRODUCTION

Recently there have been a number of publications dealing with the mechanical properties of the polymers containing glass microspheres. Such composites possess good mechanical properties and good processability at reasonable cost. Glass microspheres have also been frequently used by investigators seeking theoretical correlations for the mechanical properties of particulate-filled systems. Due to the perfect geometrical shape of glass microspheres, mathematical treatment is much easier than for other, irregular-shaped fillers. Sahu and Broutman[1] used spherical particles for finite element analysis of particulate-filled polymeric resins in order to establish the relationship between stiffness, strength, and the volume fraction of filler. Leidner and Woodhams[2] also propose a mathematical model for the strength of model composites containing spherical particles.

Fracture properties of polymeric systems filled with glass microspheres were studied by Broutman and Sahu[3] and Wambach, Trachte, and Di-Benedetto.[4] Smith[5] developed an equation relating the strain behavior of composites containing a cubic close-packed arrangement of spherical particles to the volume fraction of the spherical particles. This relationship was employed by Narkis and Nicolais[6] in the characterization of SAN polymers filled with glass beads. A similar approach was also proposed by Nielsen[7] several years later in which equations were developed for calculating the area under the stress–strain curve. Such idealized particle distributions do not represent the true situation in most filled composites and therefore need some modification for real situations.[8]

TABLE I
Tensile Strength of Polyester Resin-Glass Bead Composites[a]

Glass bead code number	Diameter, mm	Surface finish	σ_{uc} at $V_b = 0$, psi	Composite tensile strength σ_{uc},[c] psi
1721	0.354–0.177	no coating	5950	$540V_b + 5950(1 - V_b)$
2429	0.105–0.053	no coating	7071	$540V_b + 7071(1 - V_b)$
3000	0.105–0.044	no coating	8227	$540V_b + 8227(1 - V_b)$
1721	0.354–0.177	CPOI[b] coating	2300	$10100V_b + 2300(1 - V_b)$
2429	0.105–0.053	CPOI coating	5700	$10100V_b + 5700(1 - V_b)$
3000	0.105–0.044	CPOI coating	7600	$10100V_b + 7600(1 - V_b)$

[a] From reference 2.
[b] Proprietary coating (Potters Ind.) recommended for use with polyester resins.
[c] For coated beads, equations valid for $V_b \geqslant V_{b\,\min}$ (see reference 2).

Several theoretical treatments on the stress–strain behavior of particulate-filled systems have been summarized by Nielsen.[9]

In this work, equations were developed to predict the ultimate strain and the area under the stress–strain curve for particulate-filled polymers. These equations take into account deviation of real systems from linear elastic behavior.

EXPERIMENTAL

Polyester resin (Stypol 40-2364, Freeman Chemical Co.) was used in all the examples. The resin was cured with 1% Lupersol DDM (60% MEK peroxide in dimethyl phthalate) and 0.3 wt-% of cobalt naphthenate (6% solution in mineral spirits). The composites were prepared by mixing a weighed quantity of glass beads (Potters Industries Inc.) with the catalyzed resin and casting the mixture between glass plates. Further details of the preparation are given in reference 2. The experimental tensile strength relationships for these composites are summarized in Table I.

Tensile stress–strain curves were obtained on the Instron tester using a 2-in. gauge length extensometer. Cross-head speed was set at 0.05 cm/min. Izod impact strength was obtained using unnotched samples 2.5 in. × 0.5 in. × 0.15 in. There was an attempt made to use the notched samples, but the measured values were too small for comparison. The values of the ultimate strain and the area under the stress–strain curve are the average of two determinations, and the values of the Izod impact strength are the average of four determinations.

THEORETICAL TREATMENT

An earlier paper[2] described the strength behavior of polyester resin composites containing spherical glass beads. A response similar to that of discontinuous short glass fiber-filled composites is apparent in that a minimum in the composite strength is found at the low volume fractions. The minimum strength occurs at the intersection of two linear relationships,

one governing the high volume fractions of glass beads and the other governing the low volume fraction region. The experimental relationships found in this system are reproduced in Table I.

In order to obtain expressions for the elongation and the area under the stress–strain curve for particulate-filled systems, a few simplifying assumptions were made:

(a) The nonlinearity of the stress-strain curve of the composite was due to the nonlinear behavior of the matrix.

(b) The equation describing Young's modulus of the particulate filled system has the form

$$E_c/E_m = f(V_b) = c \tag{1}$$

where E_m is Young's modulus of the matrix, E_c is the Young's modulus of the composite, and V_b is volume fraction of the beads. At any particular volume fraction of filler the ratio of Young's modulus of the composite to that of the matrix is a constant. As the stiffness of the matrix decreases at high stresses, the stiffness of the composite also decreases.

(c) The ratio of the stress carried by the composite to the stress carried by the matrix for any volume fraction of filler V_b is equal to the ratio of the ultimate tensile strength of the composite to the stress carried by the matrix at the breaking point of the composite; that is,

$$\sigma_c'/\sigma_m' = \sigma_{uc}/\sigma_m \tag{2}$$

where σ_c' is the stress carried by the composite, σ_m' is the corresponding stress carried by the matrix, σ_{uc} is the ultimate strength of the composite, and σ_m is the stress carried by the matrix at the breaking point of the composite (see Fig. 1).

Assumption (a) is valid for composites in which the separation between the matrix and the filler particles is very minor, i.e., for composites with good matrix–filler adhesion or for composites with poor matrix–filler adhesion but low ultimate strain of the matrix (up to about 5%).

Assumption (b) has ample justification in many of the published papers relating to the stiffness of particulate-filled systems. For example, Einstein's equation[9] has the form

$$E_c/E_m = 1 + 2.5V_b \tag{3}$$

and Guth and Smallwood's relationship[9] also shows a constant E_c/E_m ratio when V_b is constant:

$$E_c/E_m = 1 + 2.5V_b + 14.5V_b^2. \tag{4}$$

The relationship proposed by Kerner[10] was modified by Nielsen[9] for the case of fillers which were much more rigid than the matrix to yield

$$E_c/E_m = 1 + \frac{V_b}{1 - V_b}\left(\frac{15(1 - \nu_m)}{8 - 10\nu_m}\right) \tag{5}$$

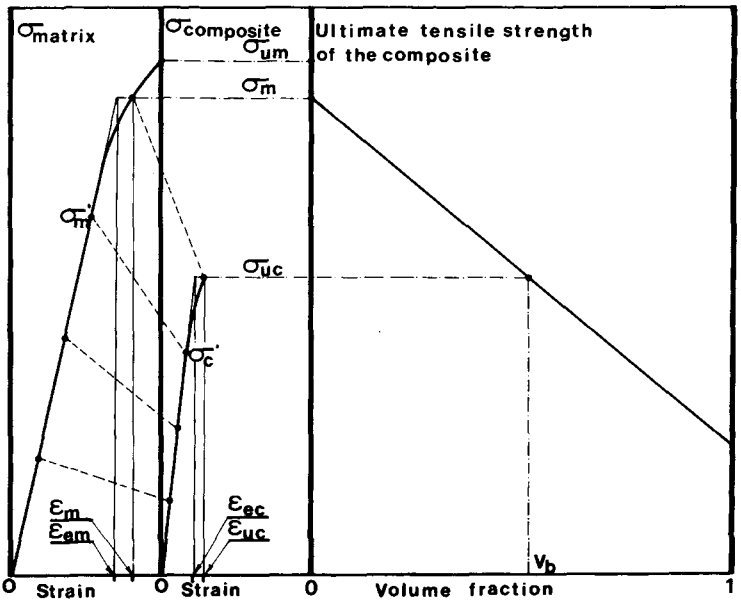

Fig. 1. Schematic representation of the assumption $\sigma_{uc}/\sigma_m = \sigma_c'/\sigma_m'$. Dashed lines show the corresponding stresses in the composite and in the matrix.

where ν_m is Poisson's ratio of the matrix. The equation proposed by Cohen and Ishai[11] simplified for the case of high-stiffness filler has the form

$$E_c/E_m = 1 + \frac{V_b}{1 - V_b^{1/3}}. \tag{6}$$

Note that all these expressions, although quite different from each other, conform to the general relationship expressed by eq. (1).

Lastly, asssumption (c) follows assumption (b). If the ratio of the moduli is constant, then the ratio of stresses is also independent of the applied stress. This is schematically illustrated by Figure 1. If the stress applied to the composite is equal σ_c', then the matrix carries a stress σ_m' The ratio between them is always equal to σ_{uc}/σ_m. This is true for ideal elastic materials, and only small deviations would be expected for most rigid thermosetting materials.

The value of the stress carried by the matrix at the breaking point of the composite can be obtained by extrapolating the line σ_{uc} versus V_b to $V_b = 0$, as shown in Figure 1 and discussed in detail in reference 2.

Ultimate Strain

Increase of the strain due to the increase in the applied stress is given by Hooke's law,

$$d\epsilon_c = d\sigma_c'/E_c \tag{7}$$

where ϵ_c is the strain of the composite. By combining eqs. (7) and (1), eq. (8) can be obtained:

$$d\epsilon_c = d\sigma_c'/E_m c. \tag{8}$$

$d\sigma_c'$ can be expressed in terms of $d\sigma_m'$ by differentiating eq. (2):

$$d\sigma_c' = \frac{\sigma_{uc}}{\sigma_m} d\sigma_m'. \tag{9}$$

After combining eqs (8) and (9) and substituting E_c/E_m for c, the expression for $d\epsilon_c$ has the form

$$d\epsilon_c = \frac{\sigma_{uc}}{\sigma_m} \frac{E_m}{E_c} \frac{d\sigma_m'}{E_m} \tag{10}$$

since

$$\sigma_{uc}/E_c = \epsilon_{ce} \tag{11}$$

and

$$\sigma_m/E_m = \epsilon_{me} \tag{12}$$

where ϵ_{ce} is the ultimate strain of the elastic material having the ultimate strength equal to σ_{uc} and a Young's modulus equal to the initial Young's modulus of the composite; ϵ_{me} is the ultimate strain of the elastic material having an ultimate strength equal σ_m and a Young's modulus the same as the initial Young's modulus of the matrix (see Fig. 1).

From Hooke's law, we obtain

$$d\sigma_m'/E_m = d\epsilon_m. \tag{13}$$

Combining eqs. (11), (12), and (13) with eq. (10), the following expression is obtained

$$d\epsilon_c = \frac{\epsilon_{ce}}{\epsilon_{me}} d\epsilon_m. \tag{14}$$

The integrated form of eq. (14) is

$$\epsilon_c = \frac{\epsilon_m}{\epsilon_{me}} \epsilon_{ce} \tag{15}$$

where ϵ_m is the strain of the matrix at a stress equal to that carried by the matrix at the fracture point of the composite.

ϵ_{ce} represents the ultimate strain of the elastic composite, and the ratio ϵ_m/ϵ_{me} represents the deviation of real systems from linear behavior.

In order to use eq. (15), ϵ_{ce} is first calculated from eq. (11), and σ_{uc} is calculated from the theory described in reference 2. E_c can be calculated from one of the eqs. (3) to (6) or from any other relationship having the form $E_c/E_m = f(V_b)$. ϵ_{me} may be obtained from eq. (12).

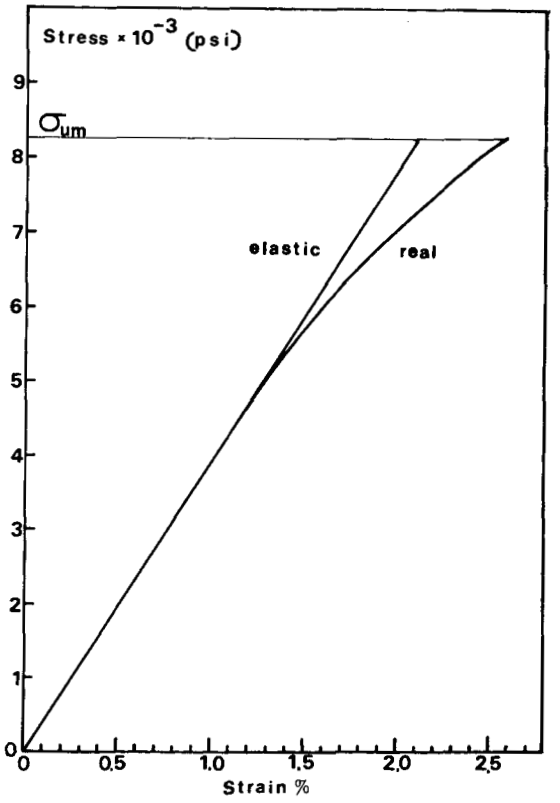

Fig. 2. Stress–strain curve of the matrix compared with the elastic behavior.

Area Under the Stress–Strain Curve

Similarly, the area under the stress–strain curve of a composite containing spherical fillers may be derived. The total energy necessary to elongate such a composite by $d\epsilon_c$ is given by the relationship

$$de_c = \sigma_c' d\epsilon_c \tag{16}$$

where e_c is the energy used to elongate the composite.

By substituting eqs (2) and (14) into eq. (16), de_c may be expressed as

$$de_c = \frac{\sigma_{uc}}{\sigma_m} \frac{\epsilon_{ce}}{\epsilon_{me}} \sigma_m' d\epsilon_m \tag{17}$$

where

$$\frac{\sigma_{uc}\epsilon_{ce}}{\sigma_m\epsilon_{me}} = \frac{e_{ce}}{e_{me}} \tag{18}$$

and

$$\sigma_m' d\epsilon_m = de_m \tag{19}$$

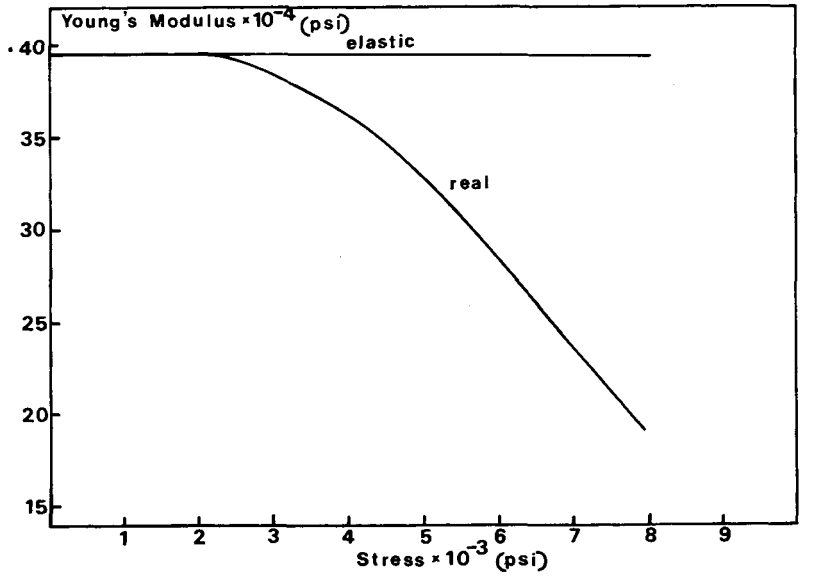

Fig. 3. Young's modulus of the matrix as a function of applied stress.

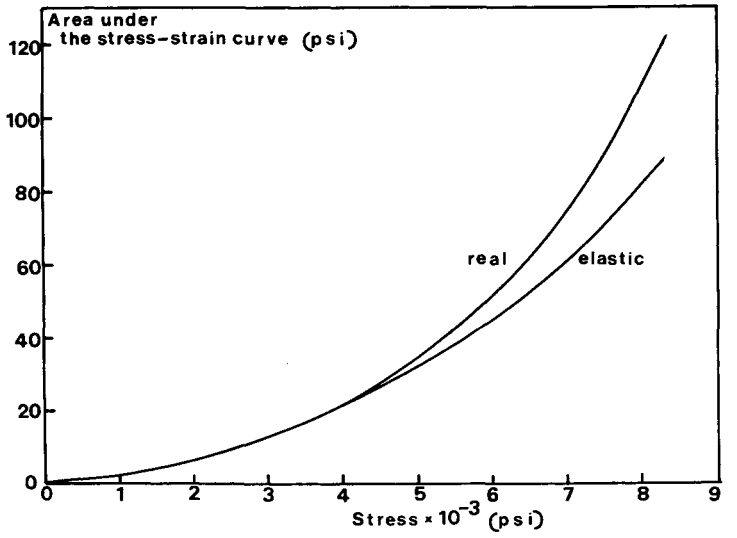

Fig. 4. Area under the tensile stress–strain curve of the matrix as a function of the applied stress, compared with the elastic behavior.

where e_{ce} is the area under the stress–strain curve for an elastic material having an ultimate strength σ_{uc} and a Young's modulus equal to that of the composite; and e_{me} is the area under the stress–strain curve for an elastic material having an ultimate strength σ_m and a Young's modulus equal to the initial Young's modulus of the matrix (see Fig. 1).

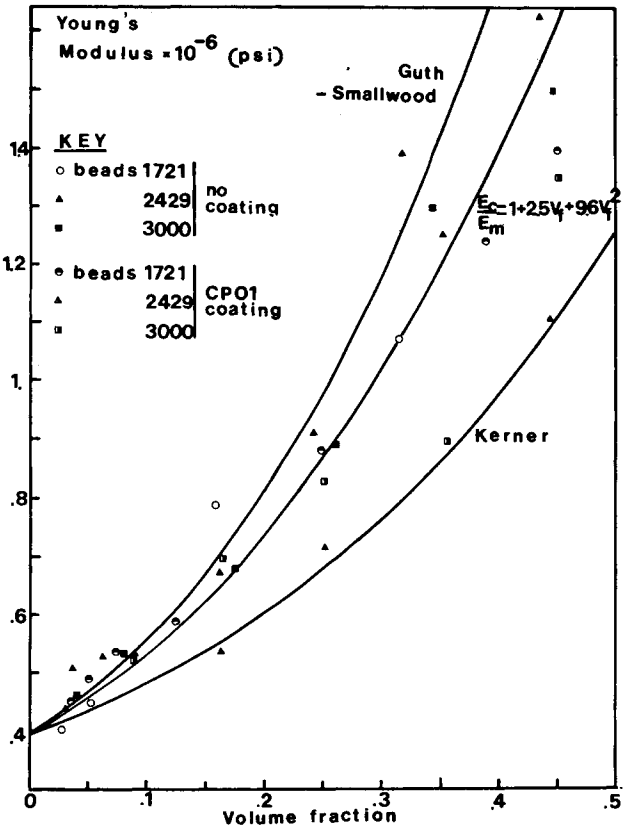

Fig. 5. Young's modulus of glass bead–polyester resin composites as a function of the volume fraction of the glass beads.

By substituting eqs. (18) and (19) into (17), an expression for de_c can be obtained:

$$de_c = \frac{e_{ce}}{e_{me}} de_m \tag{20}$$

which after integration gives

$$e_c = \frac{e_m}{e_{me}} e_{ce} \tag{21}$$

where e_{ce} represents the area under the stress–strain curve for the elastic composite and the ratio e_m/e_{me} represents the deviation of the real composite from linear behavior.

Limitations of the Theory

Equations (15) and (21) can be expected to hold well for matrices having relatively low ultimate strains (below 5%) and highly rigid, nondeformable

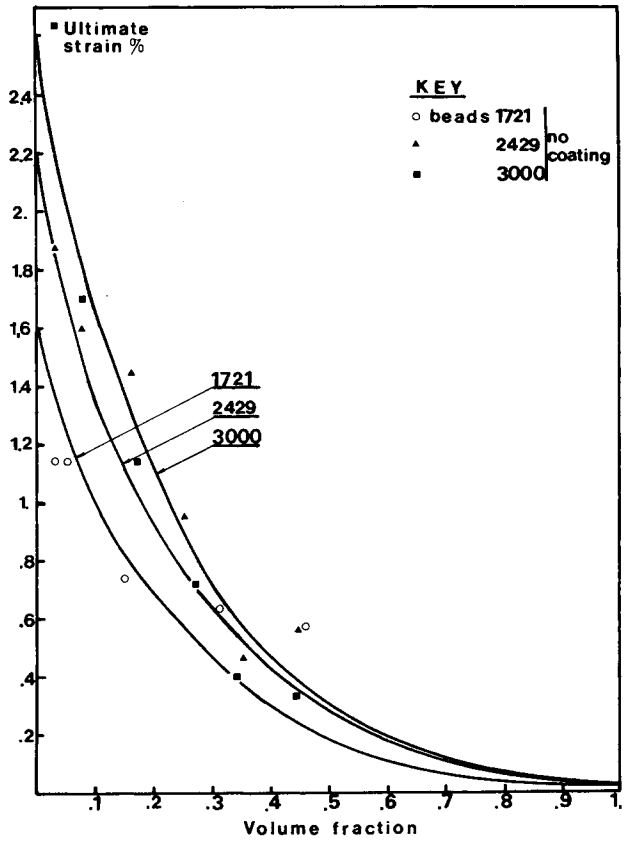

Fig. 6. Ultimate strain of the composite in the case of no adhesion between the matrix and the filler. Theoretical prediction is based on eq. (15) and the strength theory proposed in the reference 2.

fillers. Since these equations do not take into account sliding of the matrix over the surfaces of the filler particles (leading to additional elongation), they do not apply to systems where the coefficient of friction between the matrix and the filler is low (for example, when the filler is treated with a lubricant).

Equations (15) and (21) show discontinuities at $V_b = V_{b\,\min}$ due to a change in the value of σ_m (as discussed in detail in the reference 2). For real systems, a continuous transition would, of course, be expected.

RESULTS AND DISCUSSION

Figures 2, 3, and 4 characterize the matrix used in the experiments. Figure 2 shows the stress–strain curve compared with an idealized linear behavior. For stress above 5000 psi, there is a considerable deviation from linear behavior, and the ratio of ϵ_m/ϵ_{me} increases from 1 to 1.24. The modulus of the resin decreases from 396,000 psi at $\sigma_m' = 0$ to 190,000 psi

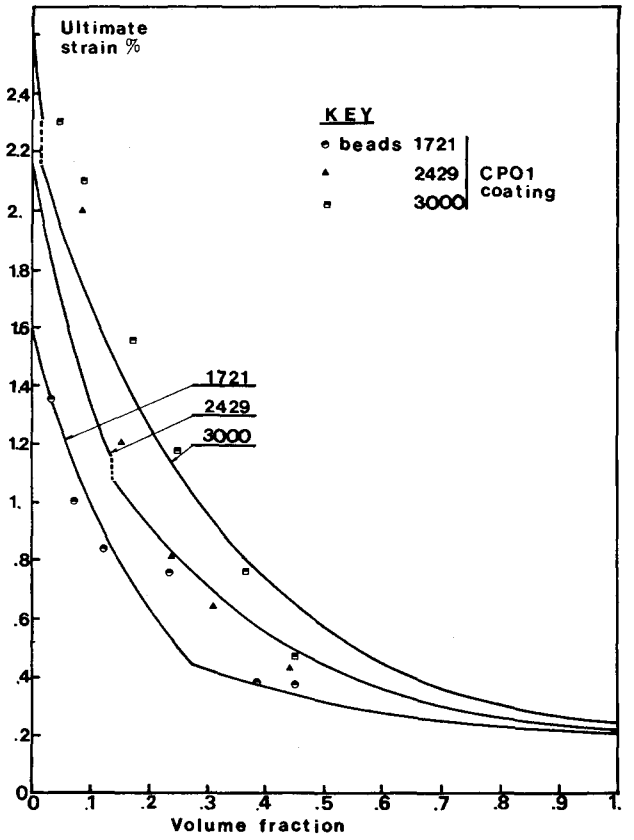

Fig. 7. Ultimate strain of the composite in case of matrix–filler adhesion. Theoretical prediction is based on eq. (15). Discontinuity in the solution occurs at $V_b = V_{b\,\min}$.

at $\sigma_m' = 8{,}000$ psi, as shown in Figure 3. Figure 4 shows the area under the stress–strain curve as a function of applied stress for this resin and in general for idealized, perfectly elastic materials. The ratio e_m/e_{me} here changes from 1 to 1.36.

Figure 5 shows the modulus of the composite as a function of volume fraction of the beads, compared with the theoretical predictions of Kerner[10] and Guth and Smallwood.[9] For this particular system, Kerner's predictions tend to define the lower bound, whereas Guth and Smallwood's results define the upper-bound values.

An empirical modification of Guth and Smallwood's equation below is closer to the mean trend although the experimental values show considerable scatter:

$$E_c/E_m = 1 + 2.5V_f + 9.6V_f^2. \tag{22}$$

Nevertheless, this equation was used for the subsequent calculations. The values of modulus appear to be independent of matrix–filler adhesion and the size of the filler particles.

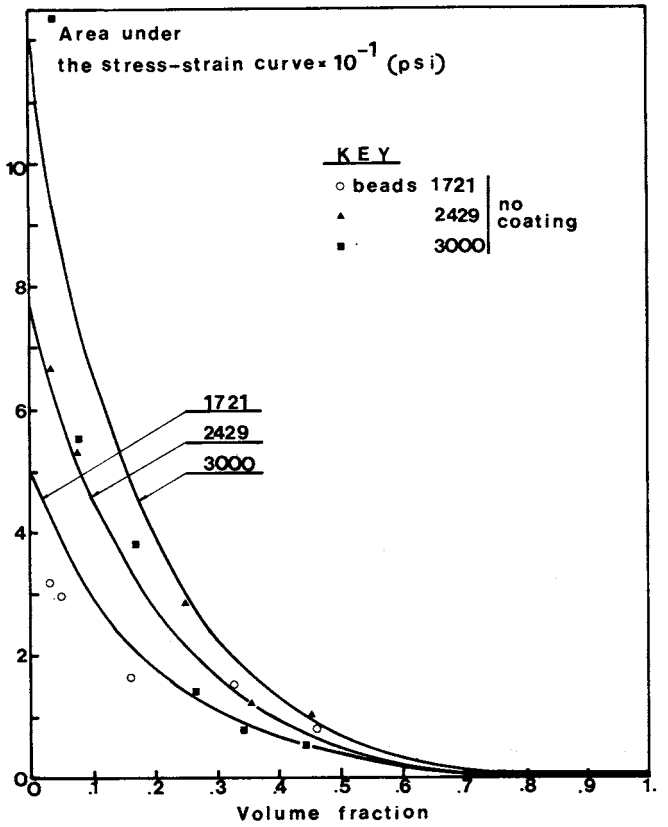

Fig. 8. Area under the stress–strain curve in case of no adhesion between the matrix and the filler. Theoretical prediction is based on eq. (21) and the strength theory proposed in reference 2.

Figure 6 shows the ultimate strain of the composite as a function of volume fraction of the beads in the case of zero adhesion between matrix and filler, whereas Figure 7 depicts the situation for good adhesion between matrix and filler. Smaller filler particles and better adhesion gave higher ultimate elongations for the composite. Composites containing fillers treated with coupling agents show higher ultimate strains than those containing untreated fillers.

The volume fraction of filler has a pronounced effect on the area under the tensile stress–strain curve for the case of zero adhesion and also good matrix–filler adhesion as shown in Figures 8 and 9, respectively. Since the area under the stress–strain curve is proportional to the ultimate strength to the second power, the results tend to be more scattered than the values of ultimate strain which have only first-power dependence on the ultimate strength. In general, predicted values tend to be higher than the experimental results.

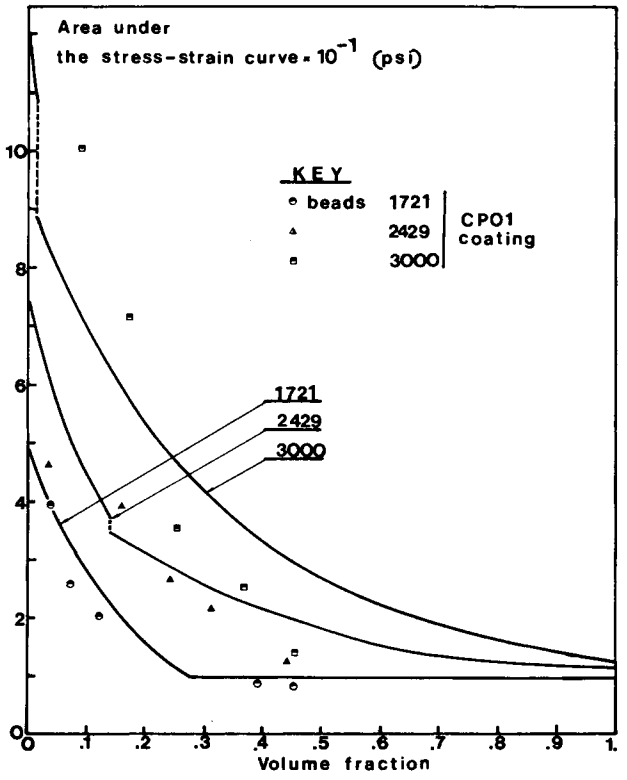

Fig. 9. Area under the stress–strain curve in case of matrix–filler adhesion. Theoretical prediction is based on eq. (21). Discontinuity in the solution occurs at $V_b = V_{b\,\min}$.

Figure 10 shows the unnotched Izod impact strength as a function of the volume fraction of the filler. The results are too scattered to draw any definite conclusions, but they seem to show the same trend as the results shown in Figures 8 and 9. Figure 11 is a plot of the area under the stress–strain curve versus the unnotched Izod impact strength. Again, the results are scattered, but the trend can be easily noticed. The greater the area under the stress–strain curve, the greater the impact strength. Such a correlation would not necessarily apply to other systems.

CONCLUSIONS

It has been suggested that the ultimate strain of a particulate-filled composite may be approximated by the relationship

$$\epsilon_c = \frac{\epsilon_m}{\epsilon_{me}} \epsilon_{ce} \tag{15}$$

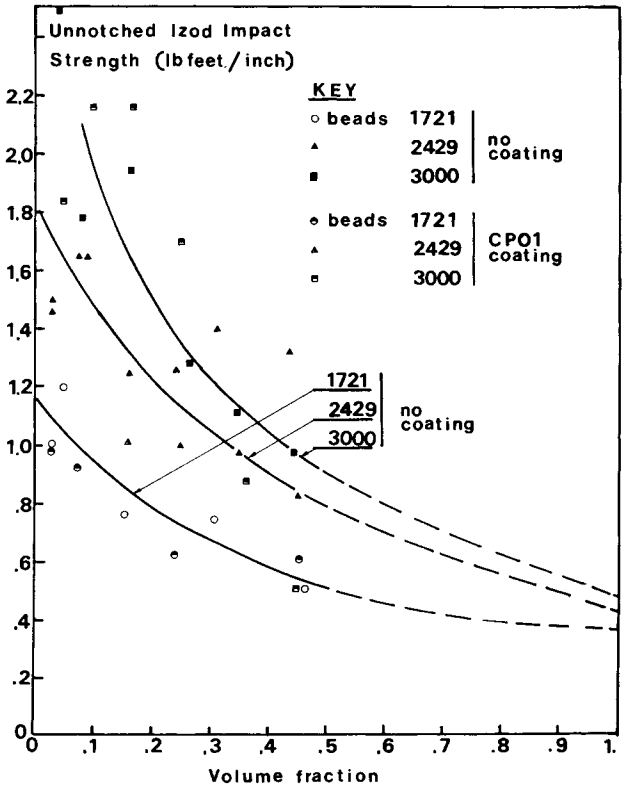

Fig. 10. Unnotched Izod impact strength as a function of the volume fraction of the filler. The curves were drawn to indicate the general trend.

and that the area under tensile stress–strain curve can be approximated by a similar equation:

$$e_c = \frac{e_m}{e_{me}} e_{ce}. \tag{21}$$

These two equations allow for an increase in the ultimate strain and the area under the stress–strain curve due to deviation of filled polymers from linear behavior.

Equations (15) and (21) which depend on the strength theory proposed in reference 2 and the appropriate modulus relationship can be used to calculate the ultimate strain and the area under the stress–strain curve. A knowledge of the area under the tensile stress–strain curve and the parameters influencing it is especially important since it is an indication of the relative toughness.

Composites containing small filler particles with good matrix–filler adhesion exhibit higher ultimate strains, larger stress–strain areas, and correspondingly greater impact strengths. Increasing the volume fraction

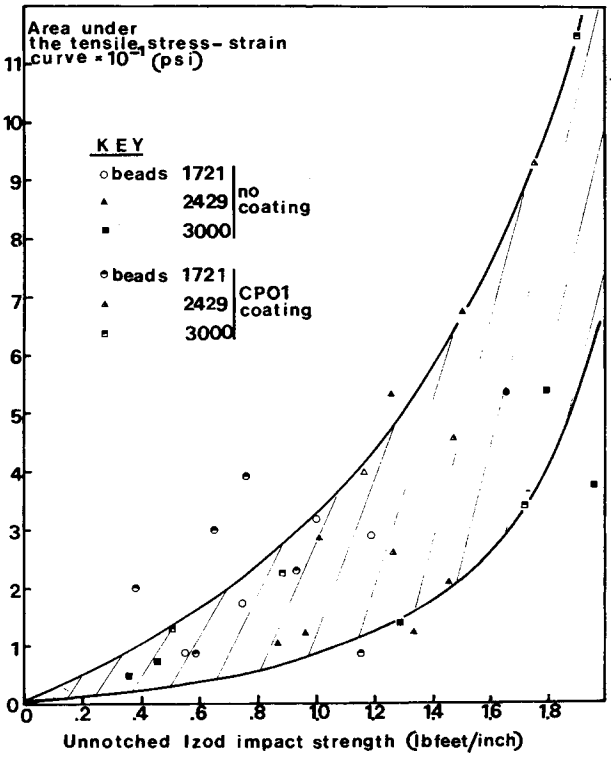

Fig. 11. Relationship between the unnotched Izod impact strength and the area under the tensile stress-strain curve.

of the filler normally decreases the ultimate elongation, the impact strength, and the area under the stress–strain curve.

This theoretical treatment assumes spherical-shaped filler particles. Further experiments would be necessary to determine whether the above approach can be applied to fillers of irregular shape.

Notation

E_c Young's modulus of the composite

E_m Young's modulus of the matrix

e_c area under the stress–strain curve of the composite

e_{ce} area under the stress–strain curve for idealized, perfectly elastic composite

e_m area under the stress–strain curve of the matrix (for σ_m' changing from 0 to σ_m)

e_{me} area under the stress-strain curve for idealized, perfectly elastic matrix (for σ_m' changing from 0 to σ_m)

V_b volume fraction of the beads

$V_{b\,\min}$ volume fraction of the filler at which the strength of the composite is minimum

ϵ_c ultimate strain of the composite
ϵ_{ce} ultimate strain of the idealized, perfectly elastic composite
ϵ_m strain of the matrix (for σ_m' changing from 0 to σ_m)
ϵ_{me} strain of the idealized, perfectly elastic matrix
σ_c' stress carried by the composite
σ_m' stress carried by the matrix
σ_{uc} ultimate strength of the composite
σ_m stress carried by the matrix at the breaking point of the composite
ν_m Poisson's ratio of the matrix

Mr. Leidner expresses his gratitude to the National Research Council of Canada for the award of a scholarship.

The research for this paper was also supported (in part) by the Defense Research Board of Canada, Grant No. 7501-08.

References

1. S. Sahu and L. Broutman, *Polym. Eng. Sci.*, **12**, 91 (1972).
2. J. Leidner and R. T. Woodhams, *J. Appl. Polym. Sci.*, **18**, 1639 (1974).
3. L. Broutman and S. Sahu, *Proc. 26th ANTEC, SPI*, **14-C**, 1 (1971).
4. A. Wambach, K. Trachte, and A. DiBenedetto, *J. Comp. Mat.*, **2**, 266 (1968).
5. T. L. Smith, *Trans. Soc. Rheol.*, **3**, 113 (1959).
6. N. Narkis and L. Nicholais, *J. Appl. Polym. Sci.*, **15**, 469 (1971).
7. L. E. Nielsen, *J. Appl. Polym. Sci.*, **10**, 97 (1966).
8. M. R. Piggott and J. Leidner, *J. Appl. Polym. Sci.*, **18**, 1619 (1974).
9. L. E. Nielsen, *J. Comp. Mat.*, **1**, 100 (1967).
10. E. H. Kerner, *Proc. Phys. Soc.*, **69B**, 808 (1956).
11. L. J. Cohen and O. Ishai, *J. Comp. Mat.*, **1**, 390 (1967).

Received January 23, 1974
Revised February 25, 1974